
K-TANH: HARDWARE EFFICIENT ACTIVATIONS FOR DEEP LEARNING

Abhisek Kundu¹ Sudarshan Srinivasan¹ Eric C. Qin² Dhiraj Kalamkar¹ Naveen K. Mellempudi¹
Dipankar Das¹ Kunal Banerjee¹ Bharat Kaul¹ Pradeep Dubey³

ABSTRACT

We propose K-Tanh, a novel, highly accurate, hardware efficient approximation of popular activation function Tanh for Deep Learning. K-Tanh consists of a sequence of parameterized bit/integer operations, such as, masking, shift and add/subtract (no floating point operation needed) where parameters are stored in a very small look-up table (bit-masking step can be eliminated). The design of K-Tanh is flexible enough to deal with multiple numerical formats, such as, FP32 and BFloat16. High quality approximations to other activation functions, e.g., Swish and GELU, can be derived from K-Tanh. We provide RTL design for K-Tanh to demonstrate its area/power/performance efficacy. It is more accurate than existing piecewise approximations for Tanh. For example, K-Tanh achieves $\sim 5\times$ speed up and $> 6\times$ reduction in maximum approximation error over software implementation of Hard Tanh. Experimental results for low-precision BFloat16 training of language translation model GNMT on WMT16 data sets with approximate Tanh and Sigmoid obtained via K-Tanh achieve similar accuracy and convergence as training with exact Tanh and Sigmoid.

1 INTRODUCTION

Recent remarkable success of Deep Learning (DL) (LeCun et al., 2015) in various application domains, such as, image classification/segmentation (using Convolutional Networks (Krizhevsky et al., 2012; He et al., 2016)), natural language translation (LSTM (Hochreiter and Schmidhuber, 1997), Transformer (Vaswani et al., 2017), ELMo (Peters et al., 2018), BERT (Devlin et al., 2019), GPT-2 (Radford et al., 2018)), playing games (AlphaGo Zero (Silver et al., 2017)) etc can be attributed to several factors (LeCun, 2019): TFLOPS processors, abundant (labeled) data sets, progress in algorithms, and user-friendly open-source libraries. With the advent of increasingly deeper and larger networks that are focused on achieving higher accuracy, the compute requirement has grown exponentially for last several years. The computation for training state-of-the-art (SOTA) DL models from 2012 (AlexNet) to 2018 (Alpha Go Zero) has been shown to increase $300,000\times$, where compute is following a doubling period of 3.43 months (Amodei and Hernandez, 2018) (Moore’s Law has an 18-month doubling period). Consequently DL models have become notoriously resource intensive and power hungry. For inference also, a trained model is deployed to make billions of predictions per day, such as, labeling/tagging of images, action recognition

in videos, speech recognition, language translation etc, consuming huge amount of power (Facebook makes 3×10^{14} inference a day (LeCun, 2019)). In fact, (Strubell et al., 2019) quantified the energy consumption, financial and environmental cost for training SOTA DL models, especially for NLP tasks, that requires weeks or months of training large networks. For example, training one Transformer model on GPU is equivalent to $300\times$ more CO₂ emission for NY \leftrightarrow SF air travel per person. (Strubell et al., 2019) concluded emphasizing on development of computationally efficient algorithms and hardware design that requires less energy. Even before such formal studies on energy profile of DL, researchers envisaged such trend and have created active research areas for efficient DL including compact models, low-precision training and/or inference (for data servers and/or embedded systems) and DL specific accelerator (non-sparse and sparse) (Jouppi, 2016; NVIDIA, 2017). (Sze et al., 2017) is a survey on these topics. Recently, (LeCun, 2019) strongly argued in favor of designing DL specific hardware driven by multiple use cases as the demand for such hardware can only grow in future.

Most of the current compute in DL can be implemented as General Matrix Multiply (GEMM) operations, and unsurprisingly the trend of efficient DL research is to optimize the GEMM kernel through software and/or hardware accelerators. Non-GEMM operations are dominated by computation of non-linear functions (activations) which are critical for non-linear representation ability of neural networks as they make neural networks capable of learning/performing complex tasks, such as, image classifications

¹Parallel Computing Labs, Intel Labs, Bangalore, India

²Georgia Institute of Technology, USA ³Parallel Computing Labs, Intel Labs, Santa Clara, USA. Correspondence to: Abhisek Kundu <abhisek.kundu@intel.com>.

and language translations. Popular choices of activations are Tanh and Sigmoid functions for language translations, and ReLU (Nair and Hinton, 2010) for image classifications. Very recently, Swish (Ramachandran et al., 2017) and Gaussian Error Linear Units (GELUs) (Hendrycks and Gimpel, 2018) are shown to achieve higher accuracy than ReLU for image classification and NLP and speech tasks as these non-saturating activations can represent non-linear behavior more accurately than ReLU (Nwankpa et al., 2018). Implementation of Swish and GELU involves calculation of Sigmoid and Tanh. Exact computation of Tanh and Sigmoid (and Swish, GELU etc) are expensive operations as they involve computation of exponential function. With the acceleration of GEMM operations, e.g. low-precision kernels for data centers and extreme low-precision binary/ternary inference on edge devices, the percentage of time spent computing such activations will become more significant. Here we are concerned about efficient approximation of such activations while preserving the intricate non-linear regions in order to perform complex tasks accurately. Tanh and Sigmoid, on real input x , are defined as

$$\text{Tanh}(x) = \frac{e^{2x} - 1}{e^{2x} + 1} = 1 - \frac{2}{1 + e^{2x}} \in [-1, 1] \quad (1)$$

$$\text{Sigmoid}(x) = 1/(1 + e^{-x}) \in [0, 1] \quad (2)$$

Sigmoid can be derived from Tanh and vice versa as follows:

$$\text{Sigmoid}(x) = (1 + \text{Tanh}(x/2))/2, \quad (3)$$

$$\text{Tanh}(x) = 2 \cdot \text{Sigmoid}(2 \cdot x) - 1. \quad (4)$$

Swish function on input x is defined as

$$\text{Swish}(x) = x \cdot \text{Sigmoid}(x) = x \cdot (1 + \text{Tanh}(x/2))/2 \quad (5)$$

Let $\Phi(x)$ be the standard Gaussian CDF on input x . $\text{GELU}(x) = x \cdot \Phi(x)$, and can be approximated as

$$\text{GELU}(x) \approx \frac{x}{2}(1 + \text{Tanh}(\sqrt{2/\pi}(x + 0.044715x^3))) \quad (6)$$

Several techniques exist to make these activations computationally efficient. One solution is to use low-precision inputs, e.g. BFloat16 (Kalamkar et al., 2019; Dillon et al., 2017), to such functions in order to achieve high-performance activations at the cost of lower accuracy. Other approaches involve software optimizations through polynomial approximations (Banerjee et al., 2019), such as, padé rational polynomials, piecewise minimax polynomials, and Taylor expansions. The third approach is to use piecewise linear approximations that are amenable to hardware design. Popular such methods are Hard Tanh/Sigmoid, Ultra-fast Tanh/Sigmoid and their variants (Theano, 2017; Abdelouahab et al., 2017). For Hard Tanh/Sigmoid, the function is split into three piecewise linear segments. Hard Tanh is defined as:

$$\text{Hard Tanh}(x) = \begin{cases} -1, & x < -1 \\ x, & -1 \leq x \leq 1 \\ 1, & x > 1 \end{cases} \quad (7)$$

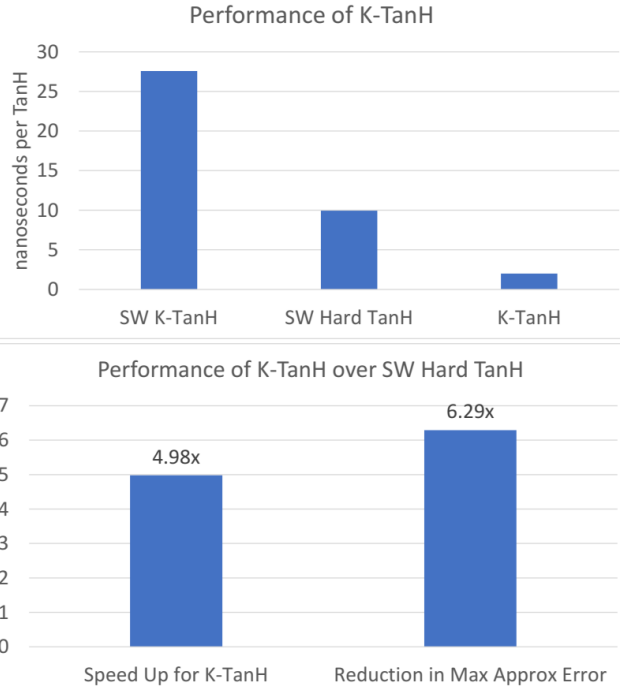


Figure 1. Performance of K-TanH: Software K-TanH is not as fast as Hard TanH. However, Hardware implementation of K-TanH is significantly faster than software Hard TanH while reducing the maximum approximation error by more than 6x.

Being the simplest piecewise linear approximation, Hard Tanh is expected to be the fastest, although it incurs significant loss of accuracy as it is a poor approximation to the Tanh curve.

1.1 Contributions

We propose a novel algorithm, namely K-TanH (Algorithm 1), to approximate Tanh using only bit/integer operations in order to achieve higher accuracy than existing piecewise linear techniques (details in Section 2). Due to the piecewise nature (determining range of inputs) of the algorithm, it may not be as fast as the fastest approximation Hard Tanh on software. However, we provide Register Transistor Level (RTL) design of K-TanH (details in Section 2) to show that it is amenable to efficient hardware implementation (Figure 1). Also, high quality approximation of other activation functions can be derived efficiently from K-TanH. We summarize our contributions as follows:

- K-TanH is a novel, highly accurate algorithm to approximate Tanh function for Deep Learning. It is more accurate than existing piecewise approximations for Tanh.
- K-TanH uses a sequence of bit/integer operations to achieve such approximation with no use of floating point

arithmetic.

- We provide RTL design for K-TanH to show its hardware efficiency. To the best of our knowledge, we are the first to demonstrate efficacy of such specialized hardware for computation of activations.
- Design of K-TanH is flexible and it can be used for multiple data formats, such as single precision FP32 (1, 8, 23) or half precision BFloat16 (1, 8, 7) etc.
- High accuracy yet low area/power profile makes K-TanH attractive to deploy in data servers as well as in mobile/embedded devices for both training and inference.
- Experimental results for low-precision BFloat16 training of language translation model GNMT (Wu et al., 2016) on WMT16 data sets with approximate Tanh and Sigmoid obtained via K-TanH achieve similar accuracy and convergence as the training with exact Tanh and Sigmoid.

In Section 2, we provide the details of K-TanH algorithm. Experimental results are shown in Section 3. In Appendix, we present Algorithm K*-TanH that simplifies K-TanH.

2 K-TANH: ACCURATE, HARDWARE EFFICIENT APPROXIMATION OF TANH

Deep Learning models are observed to be resistant to small perturbations. For Deep Learning applications, there exist several approximation methods to eliminate the computationally expensive exponentiation of Tanh and Sigmoid. These methods incur various level of loss of accuracy due to approximation. Here we investigate some of them.

2.1 Existing Approximation of Tanh/Sigmoid

2.1.1 Hard Tanh and Hard Sigmoid

For Hard Tanh/Sigmoid, the function is split into three piecewise linear segments. Hard Sigmoid is defined as:

$$\text{Hard Sigmoid}(x) = \max(0, \min(1, m \cdot x + c)) \quad (8)$$

where $c = 0.5$, and slope $m = 0.25$.

2.1.2 Hard Tanh Theano

Theano (Theano, 2017) implements Hard Sigmoid with slope $m = 0.2$ and $c = 0.5$. This method needs a float multiplication as $y = m \cdot x + c$. We can derive Hard Tanh from this using 4.

2.1.3 Ultra-fast Tanh

Ultra-fast Tanh/Sigmoid is more refined approximation than Hard Tanh/Sigmoid as it produces five piece-wise linear

Algorithm 1 K-TanH

1. **Input:** Input Exponent E_{in} , Exponent Bias E_b , Input Mantissa M_{in} , Parameter Table \mathcal{T} .
 2. **Output:** Output Exponent E_{out} , Output Mantissa M_{out}
 3. **Case I:** $E_{in} > E_b$
 4. $E_{out} \leftarrow E_b, M_{out} \leftarrow 0$. /* Output is $\text{sign}(x) \cdot 1$ */
 5. **Case II:** $E_{in} = E_b$
 6. $E_{out} \leftarrow E_{in} - 1$;
 7. Decode 2 MSBs of M_{in} ; /* Four cases */
 8. For each of four cases:
 9. Read parameters $\mathcal{P} \leftarrow (R0, S0, T0, B0, A0)$ from \mathcal{T}
 10. $M_{out} \leftarrow$ Perform bit-AND, bit-OR, bit-Shift, and bit-ADD on M_{in} using \mathcal{P}
 11. **Case III:** $E_{in} = E_b - 1$
 12. $E_{out} \leftarrow E_{in}$;
 13. Decode 2 MSBs of M_{in} ; /* Four cases */
 14. For each of four cases:
 15. Read parameters $\mathcal{P} \leftarrow (T0, B0, A0)$ from \mathcal{T}
 16. $M_{out} \leftarrow$ Perform bit-Shift and bit-ADD on M_{in} using \mathcal{P}
 17. **Case IV:** $E_{in} < E_b - 1$
 18. $E_{out} \leftarrow E_{in}, M_{out} \leftarrow M_{in}$ /* Output is Input */
-

segments. Ultra-fast Tanh is typically defined as

$$\text{Ultra Tanh}(x) = \begin{cases} \text{sign}(x) \cdot 1, & |x| > T_2 \\ m_1 \cdot x + \text{sign}(x) \cdot c_1, & T_1 < |x| \leq T_2 \\ x, & |x| < T_1 \end{cases}$$

2.1.4 APB Tanh (Abdelouahab et al., 2017)

(Abdelouahab et al., 2017) used a variant of Ultra-fast Tanh where $m_1 = 0.5, c_1 = 0.25, T_1 = 0.5, T_2 = 1.5$. This approximation of Tanh uses floating point comparators to determine the range of inputs and produces output accordingly. Here $m_1 \cdot x$ might be easy to compute without multiplication.

2.2 K-TanH: Our Algorithm to Approximate Tanh

We propose a novel algorithm for peicewise non-linear approximation of Tanh function using a sequence of only bit/integer operations, such as, bit-masking, bit-shift, and bit-add/subtract. These operations are parameterized where the parameter values are encoded in small look-up tables (LUT). Also, we need only integer comparators to determine the range of input values. For deep learning, FP32 (1,8,23) and other 16-bit low-precision representations, such as, BFloat16 (1,8,7) (Dillon et al., 2017) and FP16 (1,5,10) are used as data types for GEMM operations where FP32 being the popular accumulator data type. FP32 numbers

can be quantized to 16-bit formats before sending to lower memory in order to reduce data movement cost. Non-linear transforms can be performed on FP32 or quantized output of previous operation. We propose K-TanH (Algorithm 1) to approximate Tanh for various input formats using bit/integer operations only, eliminating the need for computing expensive exponential function and floating point operations. This can significantly improve area/power profile for K-TanH (see (Dally, Matroid Scaled Machine Learning Conference, 2019) for area/power profile for various operations).

K-TanH is compatible to generic inputs that are represented by (sign, exponent, mantissa) format. We first check the exponent to determine the range of input x . In our case, the input magnitude $|x|$ can have four ranges: $|x| < 0.5$, $0.5 \leq |x| < 1$, $1 \leq |x| < 2$, and $|x| \geq 2$. For $|x| < 0.5$, output y is input x , and for $|x| \geq 2$, output magnitude is 1 such that $y = \text{sign}(x) \cdot 1$. For other inputs, we perform a sequence of parameterized bit operations on mantissa conditioned upon the two most significant bits (MSB) of mantissa. Here is a list of parameters we use.

- R0: bit pattern to reset certain mantissa bits
- S0: bit pattern to set certain mantissa bits
- T0: how many bits of mantissa to shift right
- B0: fill-in bits after shift; $B0 \in \{0, 1\}$
- A0: bias to be added to mantissa bits

For $1 \leq |x| < 2$, we reset and set certain bits of mantissa as specified by parameters R0 and S0, respectively, followed by right shift determined by parameter T0 (fill in bits can be 0 or 1 as stored in B0). For $0.5 \leq |x| < 1$, we do not need reset and set operations; however, we need to reduce the exponent by 1 (division by 2). The sign of the output remains same as the sign of the input because $\text{Tanh}(-x) = -\text{Tanh}(x)$. Overall, we need four parameters of the form (R0,S0,T0,B0,A0) and four more of the form (T0,B0,A0) to store in the look-up table. The flow chart of Algorithm 1 is shown in Figure 2. We can use integer comparators to determine the range of inputs followed by a multiplexor for 2 MSBs of mantissa to perform LUT-based bit operations. Our algorithm is amenable to efficient hardware design for approximating Tanh function, especially for Deep Learning applications. In fact, we can use K-TanH in a quantized deep network to significantly improve its power-performance profile.

2.2.1 K-TanH for BFloat16 Inputs

We apply Algorithm 1 for BFloat16 inputs (1,8,7) where we choose the parameter values as specified in Table 1. The corresponding approximation quality is shown in Figure 3.

2.2.2 K-TanH for FP32 Inputs

For FP32 inputs (1,8,23) in Algorithm 1, we append 16 least significant ones to the parameter R0, and 16 least significant zeros to S0 and A0 of BFloat16 inputs in Table 1. Basically, we ignore the least 16 bits of mantissa while performing bit set/reset. T0 and B0 parameters are same as those of BFloat16. This way, we can use the same table for multiple input data types. The corresponding approximation quality is shown in Figure 3.

2.2.3 RTL Analysis of K-TanH for BFloat16 Inputs

K-TanH module is implemented in RTL to evaluate area, power, and performance. The conditional statements are used to describe different logic paths based on the exponent field of the BFP16 data type. LUT values are hardcoded into the design as they are read-only. The RTL design is compiled with Synopsys Design Compiler and place-and-routed with Cadence Innovus on a commercial 28nm process. The arithmetic logic and small LUT are lightweight, such that the output can be done in one cycle without any pipelining at 500 MHz. The final layout of one K-TanH module has an area overhead of 233 μm^2 and a power overhead of 0.04 mW at an activity factor of 0.2 (Figure 4).

2.3 Comparison: Quality of Approximation

Figure 5 demonstrates the high quality approximation of K-TanH despite being very efficient on hardware. We achieve $> 6\times$, $4\times$ and $\sim 2.5\times$ reduction in maximum approximation error comparing to Hard Tanh, Ultra-Fast Tanh, and APB Tanh, respectively.

2.4 Approximation of Activations using K-TanH

2.4.1 Approximating Sigmoid Activations

We can derive approximate Sigmoid from K-TanH

$$\text{Approx-Sigmoid}(x) = (1 + \text{K-TanH}(x/2))/2 \quad (9)$$

Quality of approximation of Sigmoid is shown in Figure 6 for FP32 and BFloat16 inputs.

2.4.2 Approximating Swish Activations (Ramachandran et al., 2017)

We approximate Swish using K-TanH as

$$\text{Approx-Swish}(x) = x \cdot (1 + \text{K-TanH}(x/2))/2 \quad (10)$$

Figure 8 demonstrates the quality of approximation of Swish for BFloat16 inputs. We observed similar high-quality approximation for FP32 inputs to K-TanH.

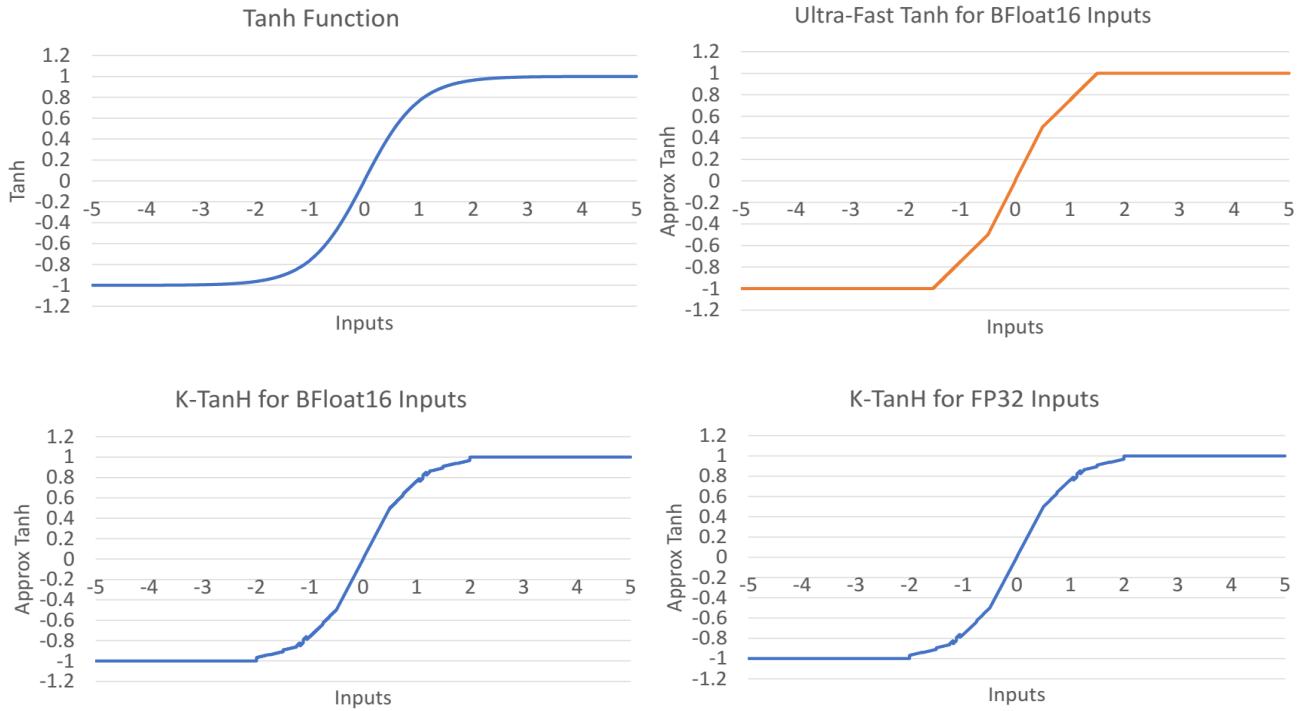


Figure 3. Approximation quality of K-TanH (Algorithm 1) for BFloat16 and FP32 inputs. K-TanH can better represent the intricate non-linear regions of Tanh than Ultra-fast APB TanH.

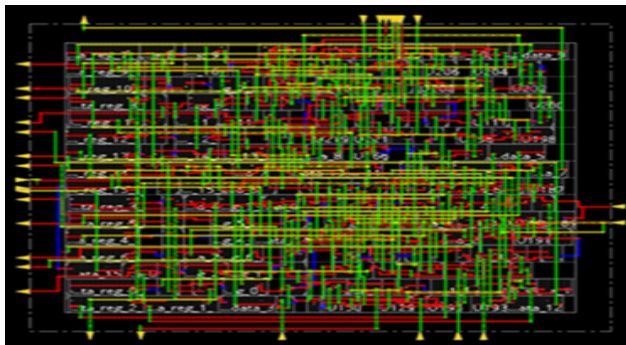


Figure 4. RTL Layout for K-TanH (Algorithm 1)

Reduction of Max Approx Error using K-TanH

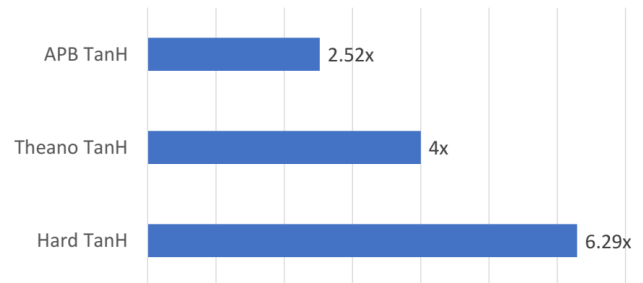


Figure 5. Reduction in maximum approximation error for computing Tanh. K-TanH is significantly more accurate than existing piecewise linear methods.

3.1.2 German to English (De-En)

We trained a 4-layer LSTM and an 8-layer LSTM on German to English data set for 50K iterations and 200K iterations, respectively. We observe similar best Bleu scores for exact activations and approximate activations using K-TanH for BFloat16 inputs for both validation and test sets (Tables 3, 4). Figures 10 and 11 show the convergence behavior for the corresponding training process.

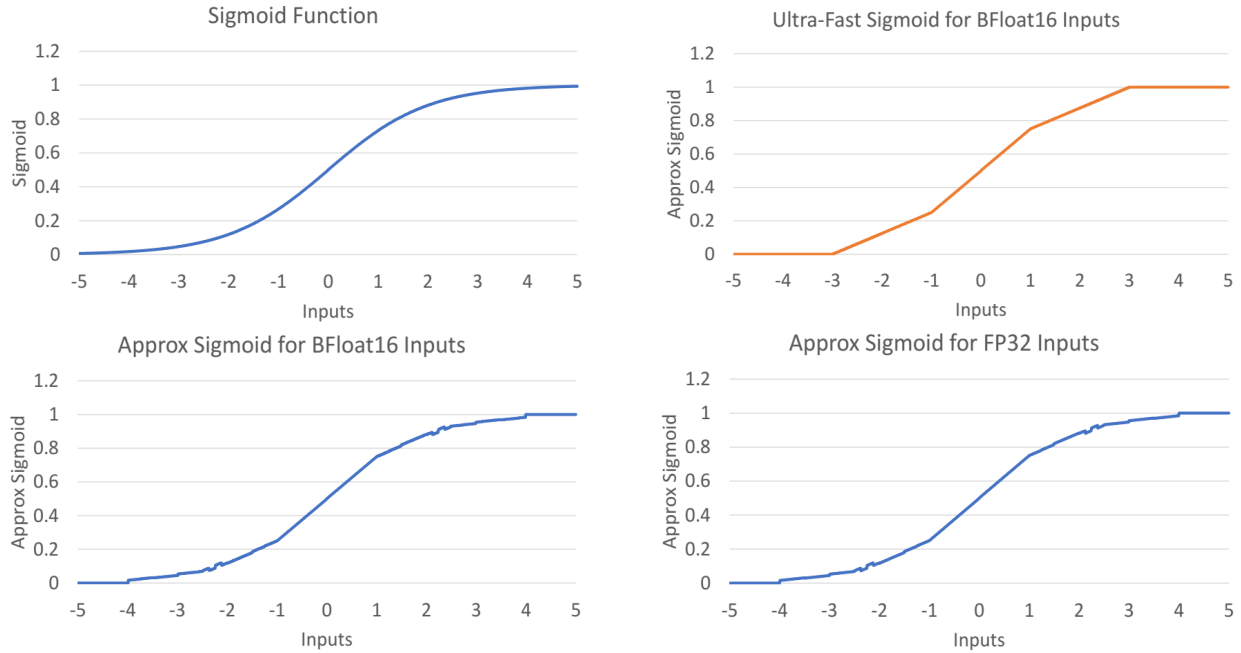


Figure 6. Approximation quality of Sigmoid using K-TanH (Algorithm 1) and equation 4 for BFloat16 and FP32 inputs. Intricate non-linear regions of Sigmoid can be better approximated by K-TanH than Ultra-Fast Sigmoid derived from APB TanH.

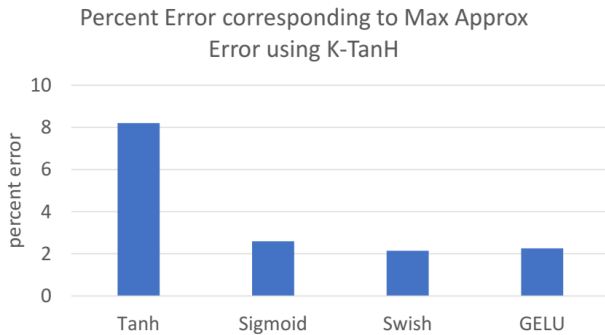


Figure 7. Approximation using K-TanH: Percentage error corresponding to the maximum approximation error using K-TanH is the highest for Tanh function. Existing piecewise linear methods are much worse than K-TanH (Figure 5).

Overall, experimental results for low-precision BFloat16 training of language translation models on GNMT data sets with approximate Tanh and Sigmoid obtained via K-TanH achieve similar accuracy and convergence as the FP32 training with exact Tanh and Sigmoid.

4 CONCLUSION

We focus on computing activations efficiently while maintaining their non-linearity for DL workloads. For this, we propose an efficient hardware design for approximating

	Exact Activation	Approx Activation
Bleu Valid	18.4	18.1
Bleu Test	20.4	20.6

Table 2. Vi-En: Best Bleu scores for validation and test data for exact activation and approximate activation using K-TanH for BFloat16 inputs.

	Exact NonLinear	Approx NonLinear
Bleu Valid	22.7	22.8
Bleu Test	22.6	22.9

Table 3. 4-layer De-En: Best Bleu scores for validation and test data for exact activation and approximate activation for BFloat16 inputs.

	Exact NonLinear	Approx NonLinear
Bleu Valid	26.6	27
Bleu Test	27.2	27.9

Table 4. 8-layer De-En: Best Bleu scores for validation and test set for exact activations and approximate activations for BFloat16 inputs (210K iterations).

Tanh (for its ubiquitous presence as activation). Our algorithm K-TanH requires very little area and power as it uses simple logic elements involving bit/integer operations while preserving the non-linearity of such functions. Low-precision BFloat16 training on GNMT using K-TanH shows SOTA accuracy and convergence on Vi-En and De-En lan-

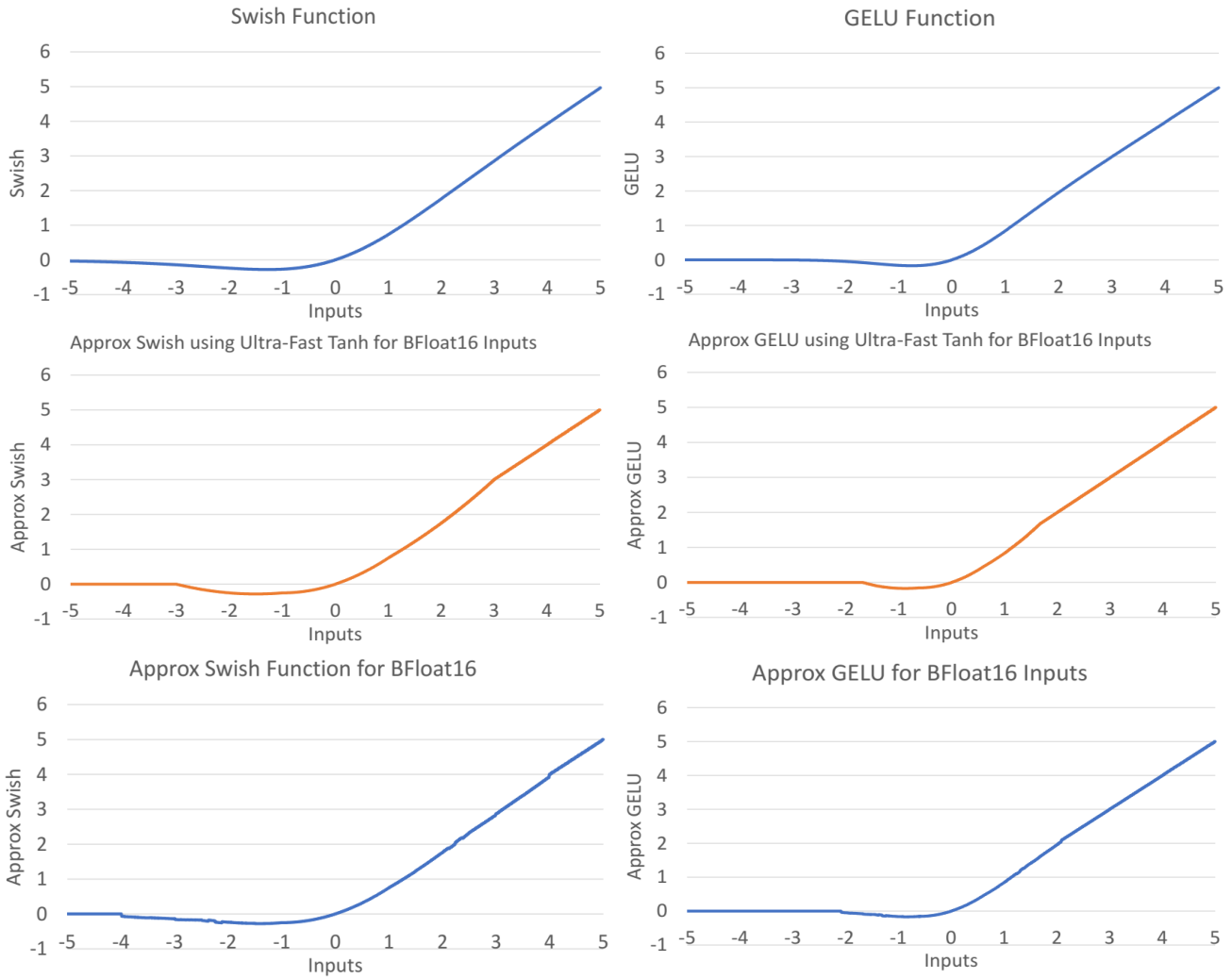


Figure 8. Approximation quality of Swish and GELU activations using K-TanH for BFloat16. High quality approximation of K-TanH helps better preserving the intricate non-linearity of Swish and GELU.

guage translation tasks. Accuracy plots for other activations, derived using K-TanH, make us believe in achieving similar results for other DL workloads. The entries of the parameter table in Table 1 are derived empirically. It would be interesting to find optimal parameter values for K-TanH.

K-TanH: Hardware Efficient Activations for Deep Learning

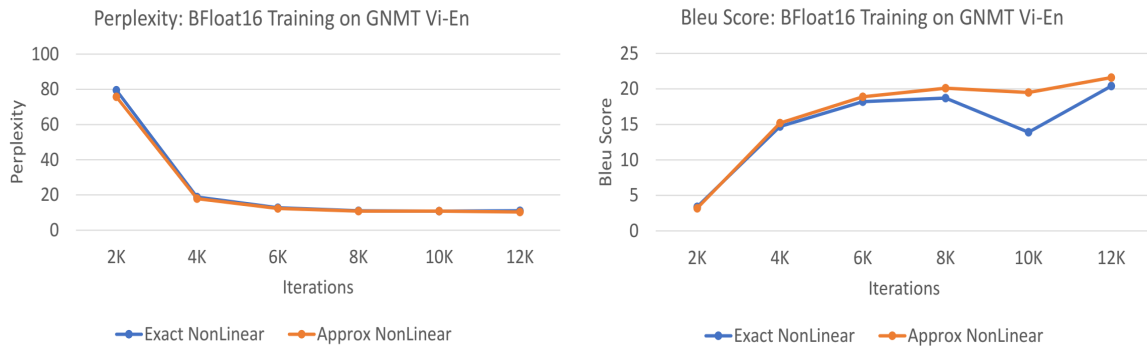


Figure 9. Vi-En: Perplexity scores and Bleu scores for training 2-layer LSTM with BFloat16 inputs. K-TanH is used to approximate both Tanh and Sigmoid functions. K-TanH shows similar accuracy as exact Tanh and Sigmoid to achieve closely matching Perplexity and Bleu scores.

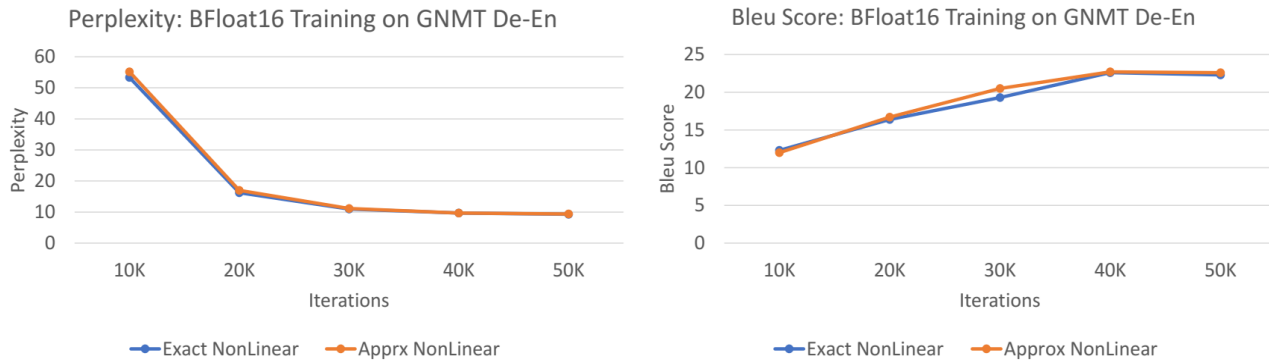


Figure 10. 4-layer De-En: Perplexity scores and Bleu scores for training 4-layer LSTM with BFloat16 inputs. K-TanH is used to approximate both Tanh and Sigmoid functions and these approximations achieve near-identical Perplexity and Bleu scores as the exact Tanh and Sigmoid.

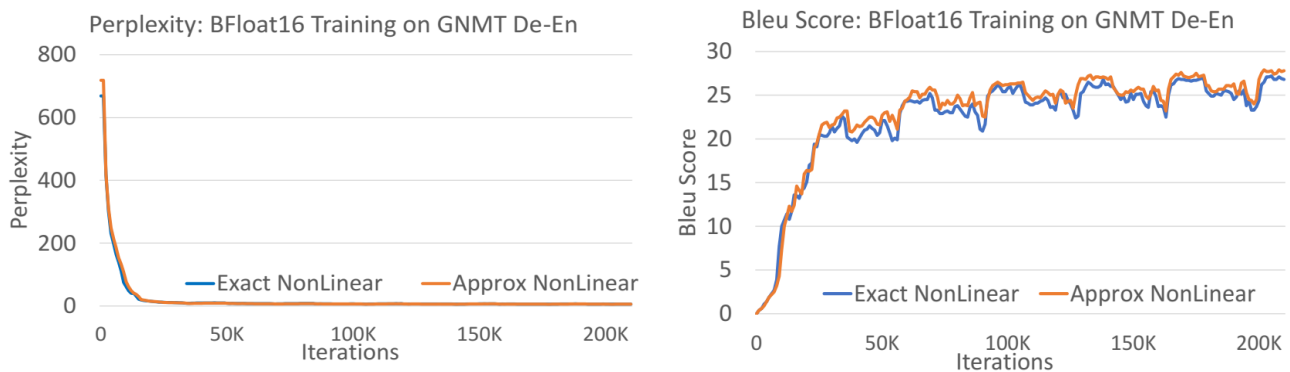


Figure 11. 8-layer De-En: Perplexity scores and Bleu scores for training 8-layer LSTM with BFloat16 inputs where K-TanH is used to approximate both Tanh and Sigmoid functions. K-TanH based results closely match (if not slightly better than) the results for exact Tanh and Sigmoid for BFloat16.

REFERENCES

- Kamel Abdelouahab, Maxime Pelcat, and Francois Berry. Phd forum: Why tanh is a hardware friendly activation function for cnns. *Proceedings of the 11th International Conference on Distributed Smart Cameras*, pages 199–201, 2017.
- Dario Amodei and Danny Hernandez. Ai and compute. <https://openai.com/blog/ai-and-compute/>, 2018.
- Kunal Banerjee, Evangelos Georganas, Dhiraj D. Kalamkar, Barukh Ziv, Eden Segal, Cristina Anderson, and Alexander Heinecke. Optimizing deep learning rnn topologies on intel architecture. *Supercomputing Frontiers and Innovations*, page (to appear), 2019.
- Bill Dally. Accelerating ai. https://www.youtube.com/watch?v=EkHnyuW_U7o&feature=youtu.be, Matroid Scaled Machine Learning Conference, 2019.
- Jacob Devlin, Ming-Wei Chang, Kenton Lee, and Kristina Toutanova. Bert: Pre-training of deep bidirectional transformers for language understanding. <https://arxiv.org/abs/1810.04805>, 2019.
- Joshua V. Dillon, Ian Langmore, Dustin Tran, Eugene Brevdo, Srinivas Vasudevan, Dave Moore, Brian Patton, Alex Alemi, Matt Hoffman, and Rif A. Saurous. Tensorflow distributions. <https://arxiv.org/abs/1711.10604>, 2017.
- Kaiming He, Xiangyu Zhang, Shaoqing Ren, and Jian Sun. Deep residual learning for image recognition. In *Proceedings of the IEEE Conference on Computer Vision and Pattern Recognition*, pages 770–778, 2016.
- Dan Hendrycks and Kevin Gimpel. Gaussian error linear units (gelus). <https://arxiv.org/abs/1606.08415>, 2018.
- Sepp Hochreiter and Jürgen Schmidhuber. Long short-term memory. *Neural computation*, 9(8):1735–1780, 1997.
- Norm Jouppi. Google supercharges machine learning tasks with tpu custom chip. *Google Blog*, May, 18, 2016.
- Dhiraj Kalamkar, Dheevatsa Mudigere, Naveen Mellempudi, Dipankar Das, Kunal Banerjee, Sasikanth Avancha, Dharma Teja Vooturi, Natraj Jammalamadaka, Jianyu Huang, Hector Yuen, Jiyan Yang, Jongshoo Park, Alexander Heinecke, Evangelos Georganas, Sudarshan Srinivasan, Abhisek Kundu, Misha Smelyanskiy, Bharat Kaul, and Pradeep Dubey. A study of bfloat16 for deep learning training. <https://arxiv.org/abs/1905.12322>, 2019.
- Alex Krizhevsky, Ilya Sutskever, and Geoffrey E. Hinton. Imagenet classification with deep convolutional neural networks. In *Advances in neural information processing systems*, pages 1097–1105, 2012.
- Yann LeCun. Deep learning hardware: Past, present, and future. *IEEE International Solid-State Circuits Conference (ISSCC)*, pages 12–19, 2019.
- Yann LeCun, Yoshua Bengio, and Geoffrey E. Hinton. Deep learning. *Nature* <http://dx.doi.org/10.1038/nature14539>, 2015.
- Vinod Nair and Geoffrey E. Hinton. Rectified linear units improve restricted boltzmann machines. *International Conference on Machine Learning (ICML)*, 2010.
- NVIDIA. Nvidia tensor cores. <https://www.nvidia.com/en-us/data-center/tensorcore/>, 2017.
- Chigozie Nwankpa, Winifred Ijomah, Anthony Gachagan, and Stephen Marshall. Activation functions: Comparison of trends in practice and research for deep learning. <https://arxiv.org/abs/1811.03378>, 2018.
- Matthew E. Peters, Mark Neumann, Mohit Iyyer, Matt Gardner, Christopher Clark, Kenton Lee, and Luke Zettlemoyer. Deep contextualized word representations. *NAACL*, 2018.
- Alec Radford, Jeffrey Wu, Rewon Child, David Luan, Dario Amodei, and Ilya Sutskever. Language models are unsupervised multitask learners. *Technical Report, OpenAI*, 2018.
- Prajit Ramachandran, Barret Zoph, and Quoc V. Le. Searching for activation functions. <https://arxiv.org/abs/1710.05941>, 2017.
- David Silver, Julian Schrittwieser, Karen Simonyan, Ioannis Antonoglou, Aja Huang, Arthur Guez, Thomas Hubert, Lucas Baker, Matthew Lai, Adrian Bolton, Yutian Chen, Timothy Lillicrap, Fan Hui, Laurent Sifre, George van den Driessche, Thore Graepel, and Demis Hassabis. Mastering the game of go without human knowledge. *Nature*, 550:354–359, 2017.
- Emma Strubell, Ananya Ganesh, and Andrew McCallum. Energy and policy considerations for deep learning in nlp. <https://arxiv.org/abs/1906.02243>, 2019.
- Vivienne Sze, Yu-Hsin CHen, Tien-Ju Yang, and Joel Emer. Efficient processing of deep neural networks: A tutorial and survey. <https://arxiv.org/abs/1703.09039>, 2017.

Theano. Theano manual on tanh and sigmoid. <https://github.com/Theano/Theano/blob/38a6331ae23250338290e886a72daadb33441bc4/theano/tensor/nnet/sigm.py#L279>, 2017.

Ashish Vaswani, Noam Shazeer, Niki Parmar, Jakob Uszkoreit, Llion Jones, Aidan N. Gomez, Łukasz Kaiser, and Illia Polosukhin. Attention is all you need. *Conference on Neural Information Processing Systems*, 2017.

Yonghui Wu, Mike Schuster, Zhifeng Chen, Quoc V. Le, Mohammad Norouzi, and et al. Googles neural machine translation system: Bridging the gap between human and machine translation. <https://arxiv.org/pdf/1609.08144.pdf>, 2016.

5 APPENDIX

5.1 K*-TANH: Improving on K-TANH

We show that K-TanH (Algorithm 1) can be modified to get rid of bit-masking step, resulting in a simplified circuit and smaller LUT (Figure 12). The new algorithm, K*-TANH, is presented as Algorithm 2 and we can use various parameter tables for Algorithm 2, such as, \mathcal{T}_1 (Table 5) and \mathcal{T}_2 (Table 6).

Using \mathcal{T}_1 , for input magnitude $x \in [1, 2)$, we shift the mantissa 2 steps and add suitable bias to it, whereas, using \mathcal{T}_2 , for input magnitude $x \in [1, 1.25)$, we only add bias with no shift. For $x \in [0.5, 1)$, we shift the mantissa 1 step with appropriate bias for both \mathcal{T}_1 and \mathcal{T}_2 .

Mathematically, these operations give us piece-wise approximations as follows. $x \in [1, 2)$, can be written as $x = 1 + 0.f$. Output of K*-TanH (assuming 7-bit mantissa), using \mathcal{T}_1 ,

$$\begin{aligned} y &\approx (1 + 0.f/2^{T_0} + A_0/2^7)/2 \\ &= x/8 + (A_0 + 96)/256 \end{aligned}$$

Therefore, K*-TanH approximates Tanh curve for this range of inputs by a line segment of slope 1/8 and the biases are retrieved from the LUT. However, using \mathcal{T}_2 , for $x \in [1, 1.25)$,

$$\begin{aligned} y &\approx (1 + 0.f + A_0/2^7)/2 \\ &= x/2 + A_0/256 \end{aligned}$$

So, this range of inputs are approximated by a line segment with slope 1/2, along with bias $A_0/256$. Similarly, for $x \in [0.5, 1)$, $x = (1 + 0.f)/2$ and output of K*-TanH is $y \approx x/2 + (64 + A_0)/256$.

Note that, we can make the Algorithm 2 more flexible (and probably more accurate) by making the exponent adjustment parameterized (E_0), i.e., $E_{out} \leftarrow E_{in} - E_0$, for various input range. For example, for $x \in [0.5, 0.625)$, $E_{out} \leftarrow E_{in} - 1$, and perform appropriate shift/add to the mantissa.

We can derive approximation to Sigmoid, Swish and GELU using K*-TanH as earlier:

$$\text{K*-Sigmoid}(x) = (1 + \text{K*-TanH}(x/2))/2$$

$$\text{K*-Swish}(x) = x \cdot (1 + \text{K*-TanH}(x/2))/2$$

$$\text{K*-GELU}(x) \approx \frac{x}{2} (1 + \text{K*-TanH}(\sqrt{\frac{2}{\pi}}(x + c \cdot x^3)))$$

where $c = 0.044715$.

Quality of approximation for TanH, Sigmoid, Swish and GELU are shown in Figure 13.

Algorithm 2 K*-TanH

1. **Input:** Input Exponent E_{in} , Exponent Bias E_b , Input Mantissa M_{in} , Parameter Table \mathcal{T} .
 2. **Output:** Output Exponent E_{out} , Output Mantissa M_{out}
 3. **Case I:** $E_{in} > E_b$
 4. $E_{out} \leftarrow E_b, M_{out} \leftarrow 0$. /* Output is $\text{sign}(x) \cdot 1$ */
 5. **Case II:** $E_{in} = E_b$
 6. $E_{out} \leftarrow E_{in} - 1$;
 7. Decode 2 MSBs of M_{in} ; /* Four cases */
 8. For each of four cases:
 9. Read parameters $\mathcal{P} \leftarrow (T_0, A_0)$ from \mathcal{T}
 10. $M_{out} \leftarrow$ Perform bit-Shift and bit-ADD on M_{in} using \mathcal{P}
 11. **Case III:** $E_{in} = E_b - 1$
 12. $E_{out} \leftarrow E_{in}$;
 13. Decode 2 MSBs of M_{in} ; /* Four cases */
 14. For each of four cases:
 15. Read parameters $\mathcal{P} \leftarrow (T_0, A_0)$ from \mathcal{T}
 16. $M_{out} \leftarrow$ Perform bit-Shift and bit-ADD on M_{in} using \mathcal{P}
 17. **Case IV:** $E_{in} < E_b - 1$
 18. $E_{out} \leftarrow E_{in}, M_{out} \leftarrow M_{in}$ /* Output is Input */
-

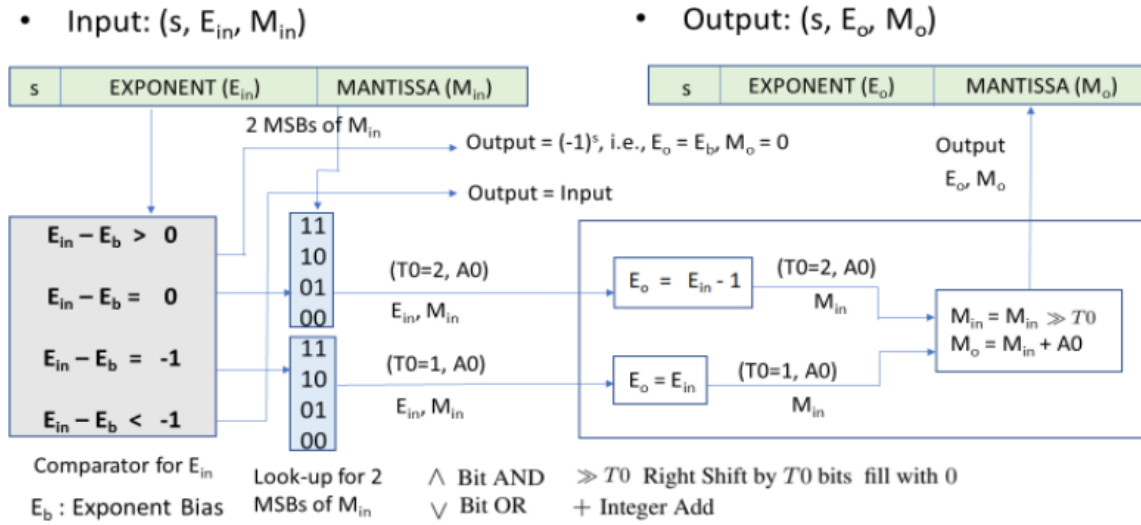


Figure 12. Flow chart for K*-TanH (Algorithm 2) to approximate Tanh computation using only bit/integer operations.

2 MSBs of M_{in}	$E_{in} = E_b$		$E_{in} = E_b - 1$	
	T0	A0	T0	A0
11	2	88	1	4
10	2	89	1	4
01	2	85	1	1
00	2	74	1	0

Table 5. Parameter table \mathcal{T}_1 for BFloat16 inputs in Algorithm 2. For FP32 inputs, we can simply append 16 least significant 0's to A0 before performing the bit operations while keeping T0 unchanged.

2 MSBs of M_{in}	$E_{in} = E_b$		$E_{in} = E_b - 1$	
	T0	A0	T0	A0
11	2	88	1	4
10	2	89	1	4
01	2	85	1	1
00	0	64	1	0

Table 6. Parameter table \mathcal{T}_2 for BFloat16 inputs in Algorithm 2. For FP32 inputs, we can simply append 16 least significant 0's to A0 before performing the bit operations while keeping T0 unchanged.

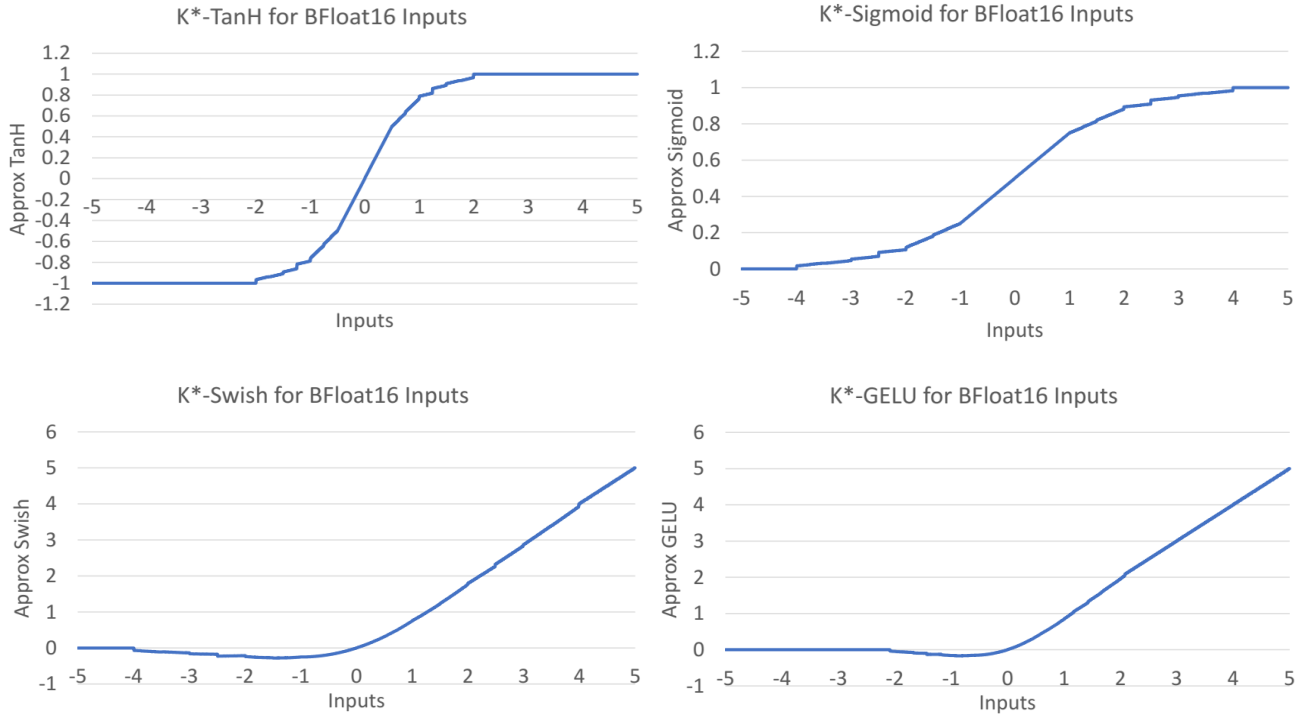


Figure 13. Approximation quality of K*-TanH (Algorithm 2) for BFloat16 inputs using parameter table \mathcal{T}_1 (Table 5).

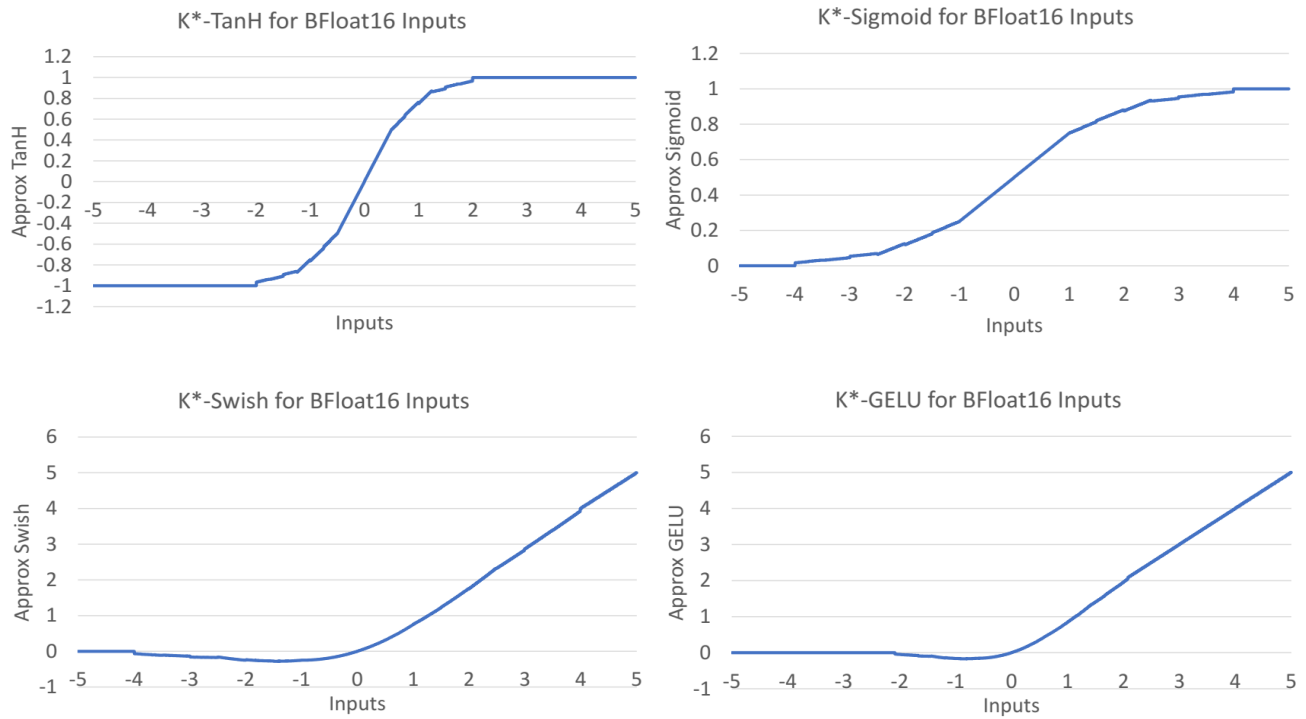


Figure 14. Approximation quality of K*-TanH (Algorithm 2) for BFloat16 inputs using parameter table \mathcal{T}_2 (Table 6).